

Partial Relaxation Approach: An Eigenvalue-Based DOA Estimator Framework

Minh Trinh-Hoang, Mats Viberg and Marius Pesavento

Abstract

In this paper, the partial relaxation approach is introduced and applied to DOA estimation using spectral search. Unlike existing methods like Capon or MUSIC which can be considered as single source approximations of multi-source estimation criteria, the proposed approach accounts for the existence of multiple sources. At each considered direction, the manifold structure of the remaining interfering signals impinging on the sensor array is relaxed, which results in closed form estimates for the interference parameters. The conventional multidimensional optimization problem reduces, thanks to this relaxation, to a simple spectral search. Following this principle, we propose estimators based on the Deterministic Maximum Likelihood, Weighted Subspace Fitting and covariance fitting methods. To calculate the pseudo-spectra efficiently, an iterative rooting scheme based on the rational function approximation is applied to the partial relaxation methods. Simulation results show that the performance of the proposed estimators is superior to the conventional methods especially in the case of low Signal-to-Noise-Ratio and low number of snapshots, irrespectively of any specific structure of the sensor array while maintaining a comparable computational cost as MUSIC.

Index Terms

DOA Estimation, Approximate Maximum Likelihood, Rank-One Modification Problem, Eigenvalue Decomposition, Least Squares Framework, Partial Relaxation, Rational Function Approximation.

I. INTRODUCTION

Direction-of-Arrival (DOA) estimation and source localization have been fundamental and long-established applications in sensor array processing. The application of DOA estimation spans multiple fields of research, including wireless communication, radio astronomy, automotive radar, etc. [1]–[4].

Many methods for DOA estimation have been developed to increase the resolution capability, computational efficiency and robustness of the algorithms. Although the family of Maximum Likelihood (ML) estimators enjoys remarkable properties of excellent threshold and asymptotic performance [5]–[7], the application of ML estimators in real-time scenarios is generally impractical due to the nonconvex optimization of a multimodal function and the associated prohibitive computational cost. In the family of subspace-based algorithms, MUSIC [8] relies on the signal subspace calculated from the spatial sample covariance matrix and performs a spectral search for the estimated DOAs. On the other hand, root-MUSIC [9], ESPRIT [10] and their unitary variants [11], [12] exploit uniform linear and shift-invariant array structures, respectively, to provide search-free DOA estimates, resulting in considerable reduction in the computational time and enhancement in the estimation performance [13]–[16].

When formulated as non-linear least squares (LS) problems, conventional spectral search algorithms ignore the existence of multiple sources in the snapshots and therefore can be regarded as single source approximation of multi-source criteria [6], [17]. As a consequence, if the interference power from other sources is high, the performance of conventional algorithms strongly degrades [5], [18]. This scenario occurs when, e.g., two or multiple sources are closely-spaced.

To overcome the aforementioned shortcomings of existing estimators without requiring specific structures of the sensor array, in this paper, DOA estimators based on the partial relaxation approach [19] are presented. Taking a fundamentally different perspective from the conventional spectral search algorithms, the partial relaxation approach takes signals from both desired and interfering directions into account. However, while the manifold structure of the desired direction is unaltered, the manifold structure of the interfering directions is relaxed to make the problem computationally tractable, hence the name partial relaxation. Based on this concept, closed-form expressions for the optimal solutions of the relaxed interference parameters are first determined and then substituted back into the multi-source criteria, resulting in simple spectral search procedures. In contrast to MUSIC, in which the eigenvectors spanning the signal subspace play an essential role in the calculation of the pseudo-spectrum, the partial relaxation approach relies only on the eigenvalues of the modified covariance matrix for each direction. In comparison to the corresponding conventional multi-source fitting methods, the partial relaxation approach admits simpler solutions while obtaining superior error performance to the conventional spectral search algorithms. To summarize, the original contributions of this paper are:

This work has been submitted to *IEEE Transactions on Signal Processing* and therefore can be withdrawn from *arXiv* without further notice.

Minh Trinh-Hoang and Marius Pesavento are with the Communication Systems Group, TU Darmstadt, Darmstadt, Germany (e-mail: thminh, pesavento@nt.tu-darmstadt.de).

Mats Viberg is with Department of Electrical Engineering, Chalmers University of Technology, Gothenburg, Sweden (e-mail: mats.viberg@chalmers.se).

- We introduce a new *Partial Relaxation Framework* for DOA estimation problem, which, from the simulation results, exhibits excellent SNR threshold performance without requiring any particular structure of the sensor array.
- We propose four new DOA estimators under the partial relaxation framework based on the classical Deterministic Maximum Likelihood, Weighted Subspace Fitting, constrained and unconstrained covariance fitting estimator.
- We propose an efficient procedure for computing the required pseudo-spectra to reduce the overall computational complexity of the partial relaxation estimators.

The paper is organized as follows. The signal model is introduced in Section II. Existing DOA methods based on non-linear least squares, which are the motivating background of the proposed work, are introduced in Section III. The mathematical formulation of the proposed partial relaxation approach and its adaptation to conventional DOA estimation methods, i.e., the Deterministic ML, Weighted Subspace Fitting, constrained and unconstrained covariance fitting estimator, are formulated in Section IV. The computational aspects of the partial relaxation framework are discussed in Section V, where the rational approximation is applied to efficiently calculate the eigenspaces and therefore avoid the full computation of the eigenvalue decomposition. To illustrate the performance gain in terms of estimation errors and execution time of the proposed methods, simulation results based on synthetic data are presented in Section VI. Lastly in Section VII, some remarks and extensions to further research are discussed.

Notation: Matrices are denoted by boldface uppercase letters \mathbf{A} , vectors are denoted by boldface lowercase letters \mathbf{a} , and scalars are denoted by regular letters a . \mathbf{I}_M represents the $M \times M$ identity matrix. Symbols $(\cdot)^H$, $(\cdot)^{-1}$, $(\cdot)^\dagger$ and $(\cdot)^{-1/2}$ denote the Hermitian transpose, inverse, Moore-Penrose pseudo-inverse and the principal square root, respectively, of the matrix argument. The expectation operator is represented by $\mathbb{E}\{\cdot\}$. The trace operator is denoted by $\text{tr}\{\cdot\}$, and the determinant is represented by $\det(\cdot)$. $\|\cdot\|_F$ denotes the Frobenius norm, and $\|\cdot\|_2$ is the ℓ_2 -norm of the argument. Finally, $\arg \min^N f(\cdot)$ denotes the N arguments for which the function $f(\cdot)$ attains its N -deepest local minima.

II. SIGNAL MODEL

Consider an array of M sensors receiving N narrowband signals emitted from the sources with the corresponding unknown DOAs $\boldsymbol{\theta} = [\theta_1, \dots, \theta_N]^T$. Furthermore, we assume that $N < M$. The sensor measurement vector $\mathbf{x}(t) = [x_1(t), \dots, x_M(t)]^T \in \mathbb{C}^{M \times 1}$ in the baseband at the time instance t is modeled as:

$$\mathbf{x}(t) = \mathbf{A}(\boldsymbol{\theta})\mathbf{s}(t) + \mathbf{n}(t) \quad \text{with } t = 1, \dots, T, \quad (1)$$

where $\mathbf{s}(t) = [s_1(t), \dots, s_N(t)]^T \in \mathbb{C}^{N \times 1}$ denotes the baseband source signal vector from N sources and $\mathbf{n}(t) \in \mathbb{C}^{M \times 1}$ represents the additive circularly complex noise vector at the sensor array with the noise covariance matrix $\mathbb{E}\{\mathbf{n}(t)\mathbf{n}(t)^H\} = \sigma_n^2 \mathbf{I}_M$. We assume that $T \geq M$. The steering matrix $\mathbf{A}(\boldsymbol{\theta}) \in \mathbb{C}^{M \times N}$ in (1), which is assumed to have full column rank is given by:

$$\mathbf{A}(\boldsymbol{\theta}) = [\mathbf{a}(\theta_1), \dots, \mathbf{a}(\theta_N)], \quad (2)$$

where $\mathbf{a}(\theta_n)$ denotes the sensor array response for the DOA θ_n . Equation (1) can be rewritten for multiple snapshots $t = 1, \dots, T$ in a compact notation as:

$$\mathbf{X} = \mathbf{A}(\boldsymbol{\theta})\mathbf{S} + \mathbf{N}, \quad (3)$$

where $\mathbf{X} = [\mathbf{x}(1), \dots, \mathbf{x}(T)] \in \mathbb{C}^{M \times T}$ is the received baseband signal matrix. In a similar manner, we define the source signal matrix $\mathbf{S} \in \mathbb{C}^{N \times T}$ and sensor noise matrix $\mathbf{N} \in \mathbb{C}^{M \times T}$ as $\mathbf{S} = [\mathbf{s}(1), \dots, \mathbf{s}(T)]$ and $\mathbf{N} = [\mathbf{n}(1), \dots, \mathbf{n}(T)]$, respectively.

Assume that the source signals and the noise are uncorrelated, the covariance matrix of the received signal $\mathbf{R} \in \mathbb{C}^{M \times M}$ is given by:

$$\mathbf{R} = \mathbb{E}\{\mathbf{x}(t)\mathbf{x}(t)^H\} = \mathbf{A}\mathbf{R}_s\mathbf{A}^H + \sigma_n^2 \mathbf{I}_M, \quad (4)$$

where $\mathbf{R}_s = \mathbb{E}\{\mathbf{s}(t)\mathbf{s}(t)^H\}$ is the covariance matrix of the transmitted signal $\mathbf{s}(t)$. In practice, the true covariance matrix \mathbf{R} is not available and the sample covariance matrix $\hat{\mathbf{R}}$ is used instead:

$$\hat{\mathbf{R}} = \frac{1}{T} \mathbf{X} \mathbf{X}^H. \quad (5)$$

Subspace techniques rely on the properties of the eigenspaces of the sample covariance matrix $\hat{\mathbf{R}}$, which is decomposed as:

$$\hat{\mathbf{R}} = \hat{\mathbf{U}} \hat{\Lambda} \hat{\mathbf{U}}^H \quad (6a)$$

$$= \hat{\mathbf{U}}_s \hat{\Lambda}_s \hat{\mathbf{U}}_s^H + \hat{\mathbf{U}}_n \hat{\Lambda}_n \hat{\mathbf{U}}_n^H. \quad (6b)$$

In (6b), $\hat{\Lambda}_s \in \mathbb{C}^{N \times N}$ is a diagonal matrix, containing the N -largest eigenvalues $\hat{\lambda}_1, \dots, \hat{\lambda}_N$, and $\hat{\mathbf{U}}_s \in \mathbb{C}^{M \times N}$ contains the corresponding N -principal eigenvectors of the sample covariance matrix $\hat{\mathbf{R}}$. Similarly, $\hat{\Lambda}_n \in \mathbb{C}^{(M-N) \times (M-N)}$ and $\hat{\mathbf{U}}_n \in \mathbb{C}^{M \times (M-N)}$ contain the $(M-N)$ -noise eigenvalues $\hat{\lambda}_{N+1}, \dots, \hat{\lambda}_M$ and the associated noise eigenvectors, respectively.

III. EXISTING METHODS BASED ON NON-LINEAR LS

In the family of ML estimators, the Deterministic ML (DML) estimates the DOAs by searching for the steering matrix \mathbf{A} in the array manifold \mathcal{A}_N , which is parameterized as follows:

$$\mathcal{A}_N = \{\mathbf{A} | \mathbf{A} = [\mathbf{a}(\vartheta_1), \dots, \mathbf{a}(\vartheta_N)], \vartheta_1 < \dots < \vartheta_N\}. \quad (7)$$

Using the parameterization in (7), the DML estimator is formulated, based on the signal model (3), as the following non-linear least squares problem [2]:

$$\{\tilde{\mathbf{A}}_{\text{DML}}, \tilde{\mathbf{S}}\} = \arg \min_{\mathbf{A} \in \mathcal{A}_N, \mathbf{S} \in \mathbb{C}^{N \times T}} \|\mathbf{X} - \mathbf{AS}\|_F^2. \quad (8)$$

In the case that only the DOAs are considered, the DML estimator in (8) can be reformulated as:

$$\{\tilde{\mathbf{A}}_{\text{DML}}\} = \arg \min_{\mathbf{A} \in \mathcal{A}_N} \text{tr} \left\{ \mathbf{P}_A^\perp \hat{\mathbf{R}} \right\}. \quad (9)$$

In (9), $\mathbf{P}_A = \mathbf{A} (\mathbf{A}^H \mathbf{A})^{-1} \mathbf{A}^H$ denotes the projection matrix onto the subspace spanned by the columns of matrix \mathbf{A} . Similarly, $\mathbf{P}_A^\perp = \mathbf{I}_M - \mathbf{P}_A$ is the projection matrix onto the orthogonal subspace spanned by the columns of matrix \mathbf{A} .

In general, the DOA estimation problem can be formulated as:

$$\{\tilde{\boldsymbol{\theta}}\} = \arg \min_{\mathbf{A}(\boldsymbol{\theta}) \in \mathcal{A}_N} f(\mathbf{A}(\boldsymbol{\theta})), \quad (10)$$

where $\tilde{\boldsymbol{\theta}}$ denotes the vector of DOA estimates and $f(\cdot)$ is a properly chosen cost function, which depends on the criteria considered for the DOA estimation task. Since the array manifold \mathcal{A}_N is highly structured and non-convex, the optimization problem in (10) is generally challenging [20]–[22]. To relieve the high computational cost, a common approach is to consider (10) in a special case: the single source scenario [17], [23]. In this approach, instead of searching directly on \mathcal{A}_N , we assume that the scenario consists of a single source, and thus the steering matrix reduces to $\mathbf{A} = \mathbf{a}(\boldsymbol{\theta}) \in \mathcal{A}_1$. Then the location of N -highest peaks of the pseudo-spectrum $F(\boldsymbol{\theta})$, which is the inverse of the objective function $f(\mathbf{a}(\boldsymbol{\theta}))$ in (10), correspond to the estimated DOAs. The above mentioned steps can be compactly summarized as follows:

$$\{\tilde{\boldsymbol{\theta}}\} = \arg \min_{\mathbf{a}(\boldsymbol{\theta}) \in \mathcal{A}_1} f(\mathbf{a}(\boldsymbol{\theta})). \quad (11)$$

where the N -highest peaks can be determined by performing a grid search of N_G points on the angle-of-view. From now on, unless we want to emphasize the dependence of the steering vector $\mathbf{a}(\boldsymbol{\theta})$ on the direction, the argument $\boldsymbol{\theta}$ will be omitted. Under the single source assumption, conventional spectral-search DOA estimators from the literature are retrieved by considering different optimizing criteria [17]:

- **Measurement Fitting:** Using the formulation of the DML in (9) on the one dimensional search, the following optimization problem is obtained:

$$\{\tilde{\boldsymbol{\theta}}\} = \arg \min_{\mathbf{a} \in \mathcal{A}_1} \text{tr} \left\{ \mathbf{P}_a^\perp \hat{\mathbf{R}} \right\}. \quad (12)$$

Note that the objective function in (12) is the null-spectrum of the conventional beamformer [2].

- **Weighted Subspace Fitting (WSF):** In accordance with the DML method, the optimization problem for the Weighted Signal Subspace Fitting is formulated in [20] as:

$$\{\tilde{\mathbf{A}}\} = \arg \min_{\mathbf{A} \in \mathcal{A}_N} \text{tr} \left\{ \mathbf{P}_A^\perp \hat{\mathbf{U}}_s \mathbf{W} \hat{\mathbf{U}}_s^H \right\}, \quad (13)$$

where $\mathbf{W} \in \mathbb{C}^{N \times N}$ is a positive semidefinite weighting matrix. In [20], the authors showed that by choosing the weighting matrix as:

$$\mathbf{W} = \hat{\mathbf{\Lambda}}^2 \hat{\mathbf{\Lambda}}_s^{-1} \quad (14)$$

with $\hat{\mathbf{\Lambda}} = \hat{\mathbf{\Lambda}}_s - \hat{\sigma}_n^2 \mathbf{I}_N$ and $\hat{\sigma}_n^2 = \frac{1}{M-N} \sum_{k=N+1}^M \hat{\lambda}_k$, the estimation error of the WSF method asymptotically achieves the Cramer-Rao Bound as the number of snapshots T tends to infinity. When the single source consideration is adopted, we obtain the following optimization problem:

$$\{\tilde{\boldsymbol{\theta}}\} = \arg \min_{\mathbf{a} \in \mathcal{A}_1} \text{tr} \left\{ \mathbf{P}_a^\perp \hat{\mathbf{U}}_s \mathbf{W} \hat{\mathbf{U}}_s^H \right\}. \quad (15)$$

In a special case when $\mathbf{W} = \mathbf{I}_M$, the formulation in (15) can be shown to be equivalent to the MUSIC estimator [17].

- **Covariance Fitting:** Starting from the identity in (4) and applying the least squares covariance fitting without considering the weighting matrix \mathbf{W} , we obtain [24]:

$$\left\{ \tilde{\mathbf{A}}, \tilde{\mathbf{R}}_s \right\} = \arg \min_{\mathbf{A} \in \mathcal{A}_N, \mathbf{R}_s \succeq \mathbf{0}} \left\| \hat{\mathbf{R}} - \mathbf{A} \mathbf{R}_s \mathbf{A}^H \right\|_F^2. \quad (16)$$

If the single source consideration is adopted, the optimization problem in (16) reduces to:

$$\left\{ \tilde{\boldsymbol{\theta}} \right\} = \arg \min_{\mathbf{a} \in \mathcal{A}_1} \min_{\sigma_s^2 \geq 0} \left\| \hat{\mathbf{R}} - \sigma_s^2 \mathbf{a} \mathbf{a}^H \right\|_F^2. \quad (17)$$

The inner optimization problem in (17) obtains a closed-form minimizer $\tilde{\sigma}_s^2$ given by [23]:

$$\tilde{\sigma}_s^2 = \arg \min_{\sigma_s^2 \geq 0} \left\| \hat{\mathbf{R}} - \sigma_s^2 \mathbf{a} \mathbf{a}^H \right\|_F^2 = \frac{\mathbf{a}^H \hat{\mathbf{R}} \mathbf{a}}{(\mathbf{a}^H \mathbf{a})^2}, \quad (18)$$

which is merely a scaled spectrum of the conventional beamformer. If a positive semidefinite constraint is included in the inner optimization problem in (18) as:

$$\begin{aligned} \tilde{\sigma}_s^2 &= \arg \min_{\sigma_s^2 \geq 0} \left\| \hat{\mathbf{R}} - \sigma_s^2 \mathbf{a} \mathbf{a}^H \right\|_F^2 \\ &\text{subject to } \hat{\mathbf{R}} - \sigma_s^2 \mathbf{a} \mathbf{a}^H \succeq \mathbf{0}, \end{aligned} \quad (19)$$

then the minimizer $\tilde{\sigma}_s^2$ is given by the Capon spectrum [23], [25]:

$$\tilde{\sigma}_s^2 = \frac{1}{\mathbf{a}^H \hat{\mathbf{R}}^{-1} \mathbf{a}}. \quad (20)$$

We remark that the optimization problems obtained by applying the single source approach to the least squares fitting problems in (9), (13) and (16) are equivalent to the multi-source criteria counterparts under the assumptions of orthogonal steering vectors, i.e., $\mathbf{A}^H \mathbf{A} = \mathbf{I}_M$, and uncorrelated signals sources. In this case, the effects of interfering signals on the desired direction vanish. As a result, the steering vectors are decoupled, and the multidimensional optimization problems can be decomposed into multiple single source estimation problems. Conversely, if the steering vector are not orthogonal, the performance of the single source approach degrades due to the interference of neighboring source signals.

IV. PARTIAL RELAXATION APPROACH

In order to relieve the aforementioned drawbacks of the conventional spectral-search algorithms, in this section, the general concept for the partial relaxation approach is introduced. Afterwards, four DOA estimators are proposed by adopting the partial relaxation approach on the classical least squares problems in (9), (13), (16) and (19).

A. General Concept

Unlike the single source consideration, our proposed partial relaxation approach considers the signals from both the desired and interfering directions. However, to make the problem tractable, the array structure of the interfering signal is relaxed. To be more precise, instead of enforcing the steering matrix $\mathbf{A} = [\mathbf{a}(\theta_1), \dots, \mathbf{a}(\theta_N)]$ to be an element in the highly structured array manifold \mathcal{A}_N as in (10), without the loss of generality, we maintain the manifold structure of the first column $\mathbf{a}(\theta_1)$ of \mathbf{A} , corresponding to the signal of consideration, and relax the manifold structure of the remaining sources $[\mathbf{a}(\theta_2), \dots, \mathbf{a}(\theta_N)]$ to an arbitrary matrix $\mathbf{B} \in \mathbb{C}^{M \times (N-1)}$, which are considered as interfering sources. Mathematically, we assume that $\mathbf{A} \in \bar{\mathcal{A}}_N$, where the relaxed array manifold $\bar{\mathcal{A}}_N$ is parameterized as follows:

$$\bar{\mathcal{A}}_N = \left\{ \mathbf{A} \mid \mathbf{A} = [\mathbf{a}(\vartheta), \mathbf{B}], \mathbf{a}(\vartheta) \in \mathcal{A}_1, \mathbf{B} \in \mathbb{C}^{M \times (N-1)} \right\}. \quad (21)$$

Note that $\bar{\mathcal{A}}_N$ still retains some structure regarding the geometry of the sensor array, hence the name partial relaxation. However, only one DOA can be estimated if (10) is minimized on the relaxed array manifold $\bar{\mathcal{A}}_N$ of (21). Therefore, the grid search is applied similarly to the single source consideration in Section III as follows: first we minimize the objective function in (10) with respect to \mathbf{B} , and then perform a grid search of $\mathbf{a}(\theta)$ on \mathcal{A}_1 . In the following, the partial relaxation approach is employed in the four algorithms introduced in Section III, i.e., the DML, WSF, unconstrained and constrained covariance fitting estimator.

B. Partially-Relaxed DML (PR-DML)

Adopting the partial relaxation approach on the objective function in (9) leads to the following optimization problem:

$$\{\hat{\theta}_{\text{PR-DML}}\} = {}^N \arg \min_{\mathbf{a} \in \mathcal{A}_1} \min_{\mathbf{B}} \text{tr} \left\{ \mathbf{P}_{[\mathbf{a}, \mathbf{B}]}^\perp \hat{\mathbf{R}} \right\}. \quad (22)$$

Rewriting the objective function of (22) to partially decouple \mathbf{a} and \mathbf{B} yields:

$$\text{tr} \left\{ \mathbf{P}_{[\mathbf{a}, \mathbf{B}]}^\perp \hat{\mathbf{R}} \right\} = \text{tr} \left\{ \mathbf{P}_{\mathbf{a}}^\perp \hat{\mathbf{R}} \right\} - \text{tr} \left\{ \mathbf{P}_{\mathbf{P}_{\mathbf{a}}^\perp \mathbf{B}} \hat{\mathbf{R}} \right\}, \quad (23)$$

where we use the convention that $\text{tr} \left\{ \mathbf{P}_{\mathbf{P}_{\mathbf{a}}^\perp \mathbf{B}} \hat{\mathbf{R}} \right\} = 0$ if $\mathbf{P}_{\mathbf{a}}^\perp \mathbf{B} = \mathbf{0}$. Since the first term on the right hand side of (23) does not depend on \mathbf{B} , the inner optimization problem in (22) is equivalent to:

$$\max_{\mathbf{B}} \text{tr} \left\{ \mathbf{P}_{\mathbf{P}_{\mathbf{a}}^\perp \mathbf{B}} \hat{\mathbf{R}} \right\}. \quad (24)$$

The solution of (24) is given by (see Appendix A):

$$\max_{\mathbf{B}} \text{tr} \left\{ \mathbf{P}_{\mathbf{P}_{\mathbf{a}}^\perp \mathbf{B}} \hat{\mathbf{R}} \right\} = \sum_{k=1}^{N-1} \lambda_k \left(\mathbf{P}_{\mathbf{a}}^\perp \hat{\mathbf{R}} \right), \quad (25)$$

where $\lambda_k(\cdot)$ denotes the k -th largest eigenvalue of the matrix in the argument. Substituting (23) and (25) back into the objective function of (22) and taking its inverse, the pseudo-spectrum of the PR-DML estimator is obtained as:

$$F_{\text{PR-DML}}(\theta) = \frac{1}{\sum_{k=N}^M \lambda_k(\mathbf{P}_{\mathbf{a}(\theta)}^\perp \hat{\mathbf{R}})}. \quad (26)$$

The estimated DOAs $\hat{\theta} = [\hat{\theta}_1, \dots, \hat{\theta}_N]^T$ are then determined by choosing the N -highest peaks of the pseudo-spectrum $F_{\text{PR-DML}}(\theta)$. Note that as further elaborated in Section V, the pseudo-spectrum in (26) can be efficiently computed without necessarily performing a full eigenvalue decomposition at each direction, i.e., computing the corresponding set of eigenvectors of the matrix $\mathbf{P}_{\mathbf{a}(\theta)}^\perp \hat{\mathbf{R}}$ is not required.

C. Partially-Relaxed WSF (PR-WSF)

Following similar derivation as for the PR-DML estimator in Subsection IV-B and using the mathematical formulation of the WSF estimator in (15), the optimization problem corresponding to the PR-WSF estimator reads:

$$\{\hat{\theta}_{\text{PR-WSF}}\} = {}^N \arg \min_{\mathbf{a} \in \mathcal{A}_1} \min_{\mathbf{B}} \text{tr} \left\{ \mathbf{P}_{[\mathbf{a}, \mathbf{B}]}^\perp \hat{\mathbf{U}}_s \mathbf{W} \hat{\mathbf{U}}_s^H \right\}, \quad (27)$$

and the pseudo-spectrum of the PR-WSF is calculated as:

$$F_{\text{PR-WSF}}(\theta) = \frac{1}{\sum_{k=N}^M \lambda_k(\mathbf{P}_{\mathbf{a}(\theta)}^\perp \hat{\mathbf{U}}_s \mathbf{W} \hat{\mathbf{U}}_s^H)}. \quad (28)$$

Note that in a special case when $\mathbf{W} = \mathbf{I}_M$, the proposed estimator in (27) is equivalent to the MUSIC estimator (see Appendix B). From now on, if not further specified, the weighting matrix \mathbf{W} is chosen as in (14).

D. Partially-Relaxed Constrained Covariance Fitting (PR-CCF)

To derive new estimators based on the covariance fitting problems in (18) and (19), we follow the partial relaxation approach for the array steering matrix as described above and relax $\mathbf{A} = [\mathbf{a}, \mathbf{B}]$ for an arbitrary $\mathbf{B} \in \mathbb{C}^{M \times (N-1)}$. Similarly, we partition the waveform matrix $\mathbf{S} = [\mathbf{s}, \mathbf{J}^T]^T$ in the signal model in (3) with $\mathbf{s} \in \mathbb{C}^{T \times 1}$ and $\mathbf{J} \in \mathbb{C}^{(N-1) \times T}$ to obtain:

$$\mathbf{X} = \mathbf{a}\mathbf{s}^T + \mathbf{D} + \mathbf{N}, \quad (29)$$

where $\mathbf{D} = \mathbf{B}\mathbf{J} \in \mathbb{C}^{M \times T}$ models the received signal of the remaining $(N-1)$ -sources with the relaxed array manifold structure and therefore $\text{rank}(\mathbf{D}) \leq N-1$. Furthermore, we assume that the sample covariance matrix $\hat{\mathbf{R}}$ is positive definite and the signals from other sources are uncorrelated with the signals from the direction $\mathbf{a}(\theta)$. Similar to the Capon beamformer in (19), the partially-relaxed constrained covariance fitting (PR-CCF) problem is formulated as follows:

$$\begin{aligned} \{\hat{\theta}_{\text{PR-CCF}}\} = {}^N \arg \min_{\mathbf{a} \in \mathcal{A}_1} \min_{\sigma_s^2 \geq 0, \mathbf{D}} & \left\| \hat{\mathbf{R}} - \sigma_s^2 \mathbf{a}\mathbf{a}^H - \mathbf{D}\mathbf{D}^H \right\|_F^2 \\ \text{subject to } & \hat{\mathbf{R}} - \sigma_s^2 \mathbf{a}\mathbf{a}^H - \mathbf{D}\mathbf{D}^H \succeq \mathbf{0} \\ & \text{rank}(\mathbf{D}) \leq N-1. \end{aligned} \quad (30)$$

Keeping $\{\sigma_s^2, \mathbf{a}\}$ fixed, minimizing (30) with respect to \mathbf{D} , a low-rank approximation problem is obtained as [26]:

$$\min_{\mathbf{D}} \left\| \hat{\mathbf{R}} - \sigma_s^2 \mathbf{a} \mathbf{a}^H - \mathbf{D} \mathbf{D}^H \right\|_F^2 = \sum_{k=N}^M \lambda_k^2 (\hat{\mathbf{R}} - \sigma_s^2 \mathbf{a} \mathbf{a}^H). \quad (31)$$

subject to $\text{rank}(\mathbf{D}) \leq N - 1$

By performing the eigenvalue decomposition as $\hat{\mathbf{R}} - \sigma_s^2 \mathbf{a} \mathbf{a}^H = \tilde{\mathbf{U}}_s \tilde{\Lambda}_s \tilde{\mathbf{U}}_s^H + \tilde{\mathbf{U}}_n \tilde{\Lambda}_n \tilde{\mathbf{U}}_n^H$ similarly to (6b), where $\tilde{\mathbf{U}}_s$ and $\tilde{\Lambda}_s$ contains the $(N - 1)$ -largest eigenvalues and the corresponding principal eigenvectors of $\hat{\mathbf{R}} - \sigma_s^2 \mathbf{a} \mathbf{a}^H$, a minimizer $\tilde{\mathbf{D}}$ of (31) satisfies $\tilde{\mathbf{D}} \tilde{\mathbf{D}}^H = \tilde{\mathbf{U}}_s \tilde{\Lambda}_s \tilde{\mathbf{U}}_s^H$. Moreover, $\hat{\mathbf{R}} - \sigma_s^2 \mathbf{a} \mathbf{a}^H$ and $\hat{\mathbf{R}} - \sigma_s^2 \mathbf{a} \mathbf{a}^H - \tilde{\mathbf{D}} \tilde{\mathbf{D}}^H$ have the same $(M - N)$ -smallest eigenvalues. It follows that $\hat{\mathbf{R}} - \sigma_s^2 \mathbf{a} \mathbf{a}^H$ is positive semidefinite if and only if $\hat{\mathbf{R}} - \sigma_s^2 \mathbf{a} \mathbf{a}^H - \tilde{\mathbf{D}} \tilde{\mathbf{D}}^H$ is positive semidefinite. As a consequence, an equivalent formulation of the inner problem in (30) is obtained as follows:

$$\min_{\sigma_s^2 \geq 0} \sum_{k=N}^M \lambda_k^2 (\hat{\mathbf{R}} - \sigma_s^2 \mathbf{a} \mathbf{a}^H) \quad (32)$$

subject to $\hat{\mathbf{R}} - \sigma_s^2 \mathbf{a} \mathbf{a}^H \succeq 0$.

It can be easily shown from the Weyl's inequality regarding the eigenvalues of the modified Hermitian matrix [27] and the positive semidefiniteness of $\hat{\mathbf{R}} - \sigma_s^2 \mathbf{a} \mathbf{a}^H$ that the objective function in (32) is strictly decreasing as σ_s^2 increases. Therefore, in the case that $\tilde{\sigma}_{s,C}^2$ is a minimizer of (32), the matrix $\hat{\mathbf{R}} - \tilde{\sigma}_{s,C}^2 \mathbf{a} \mathbf{a}^H$ exhibits at least one eigenvalue equal to zero. Consequently, the minimizer $\tilde{\sigma}_{s,C}^2$ is obtained as the Capon spectrum (see Appendix C):

$$\tilde{\sigma}_{s,C}^2 = \frac{1}{\mathbf{a}^H \hat{\mathbf{R}}^{-1} \mathbf{a}}. \quad (33)$$

Substitute (32) and (33) back into (30), the PR-CCF estimator returns the estimated DOAs by determining the N -highest peaks of the following pseudo-spectrum:

$$F_{\text{PR-CCF}}(\theta) = \frac{1}{\sum_{k=N}^M \lambda_k^2 \left(\hat{\mathbf{R}} - \frac{1}{\mathbf{a}(\theta)^H \hat{\mathbf{R}}^{-1} \mathbf{a}(\theta)} \mathbf{a}(\theta) \mathbf{a}(\theta)^H \right)}. \quad (34)$$

E. Partially-Relaxed Unconstrained Covariance Fitting (PR-UCF)

Comparing with the constrained version presented in Subsection IV-D, the formulation of the PR-UCF omits the positive semidefiniteness constraint to yield the following optimization problem:

$$\left\{ \hat{\theta}_{\text{PR-UCF}} \right\} = \arg \min_{\mathbf{a} \in \mathcal{A}_1} \min_{\sigma_s^2 \geq 0, \mathbf{D}} \left\| \hat{\mathbf{R}} - \sigma_s^2 \mathbf{a} \mathbf{a}^H - \mathbf{D} \mathbf{D}^H \right\|_F^2 \quad (35)$$

subject to $\text{rank}(\mathbf{D}) \leq N - 1$.

When minimizing with respect to \mathbf{D} , the minimizer $\tilde{\mathbf{D}}$ of the optimization problem in (35) is obtained as the best $(N - 1)$ -rank approximation of $\hat{\mathbf{R}} - \sigma_s^2 \mathbf{a} \mathbf{a}^H$. Hence, the inner optimization of the PR-UCF estimator for each direction $\mathbf{a} = \mathbf{a}(\theta)$ is:

$$\min_{\sigma_s^2 \geq 0} \sum_{k=N}^M \lambda_k^2 (\hat{\mathbf{R}} - \sigma_s^2 \mathbf{a} \mathbf{a}^H). \quad (36)$$

Unlike the constrained variant in (32), the minimizer of $g(\sigma_s^2) = \sum_{k=N}^M \lambda_k^2 (\hat{\mathbf{R}} - \sigma_s^2 \mathbf{a} \mathbf{a}^H)$ in (36) with respect to σ_s^2 , denoted as $\tilde{\sigma}_{s,U}^2$, does not have a closed form solution. However, a numerical solution of $\tilde{\sigma}_{s,U}^2$ can be determined by noting that the function $g(\sigma_s^2)$ is continuously differentiable, and the derivative $\frac{dg}{d\sigma_s^2}$ at an arbitrary point $\sigma_s^2 = \sigma_{s,0}^2$ is given by (see Appendix D):

$$\frac{dg}{d\sigma_s^2} \Big|_{\sigma_{s,0}^2} = - \sum_{k=N}^M \frac{2\bar{\lambda}_k(\sigma_{s,0}^2)}{\sigma_{s,0}^4 \mathbf{a}^H (\hat{\mathbf{R}} - \bar{\lambda}_k(\sigma_{s,0}^2) \mathbf{I}_M)^{-2} \mathbf{a}}, \quad (37)$$

where we introduce the following shorthand notation:

$$\bar{\lambda}_k(\sigma_{s,0}^2) = \lambda_k (\hat{\mathbf{R}} - \sigma_{s,0}^2 \mathbf{a} \mathbf{a}^H). \quad (38)$$

Note that the denominator in each summand of the expression in (37) is always positive, we observe that:

- If $\sigma_{s,0}^2 = \sigma_{s,C}^2$ where $\sigma_{s,C}^2$ is defined in (33), then $\bar{\lambda}_k(\sigma_{s,0}^2) \geq 0$ with $k = N, \dots, M$ and therefore:

$$\left. \frac{dg}{d\sigma_s^2} \right|_{\sigma_{s,C}^2} < 0. \quad (39)$$

- If $\sigma_{s,0}^2 \rightarrow \infty$, the rank-one component $-\sigma_{s,0}^2 \mathbf{a}\mathbf{a}^H$ is dominant to $\hat{\mathbf{R}}$ and thus we obtain an asymptotic result for the smallest eigenvalues $\bar{\lambda}_M(\sigma_{s,0}^2)$, which is defined in (38), as follows:

$$\lim_{\sigma_{s,0}^2 \rightarrow \infty} \frac{\bar{\lambda}_M(\sigma_{s,0}^2)}{\sigma_{s,0}^2 \|\mathbf{a}\|_2^2} = -1. \quad (40)$$

In addition, the remaining eigenvalues $\bar{\lambda}_k(\sigma_{s,0}^2)$ with $k = N, \dots, (M-1)$ are always bounded above and below thanks to the Weyl's inequality [27]. Applying this remark and the identity in (40) to (37) leads to:

$$\lim_{\sigma_{s,0}^2 \rightarrow \infty} \left. \frac{dg}{d\sigma_s^2} \right|_{\sigma_{s,0}^2} = \infty. \quad (41)$$

As a consequence, there exists a scalar $\sigma_{s,\text{right}}^2 < \infty$ such that

$$\left. \frac{dg}{d\sigma_s^2} \right|_{\sigma_{s,\text{right}}^2} > 0. \quad (42)$$

From (37), (39) and (42), we can perform a simple bisection search [28] on $\frac{dg}{d\sigma_s^2}$ in the interval $[\sigma_{s,C}^2, \sigma_{s,\text{right}}^2]$ to compute the minimizer $\sigma_{s,U}^2$ of (36). The steps to determine a search interval for the bisection search and the computation of the pseudo-spectrum of the PR-UCF estimator for each direction $\mathbf{a}(\theta)$ are summarized in Algorithm 1.

Algorithm 1 Determining the pseudo-spectrum of PR-UCF for a given DOA $\mathbf{a} = \mathbf{a}(\theta)$

```

1: Initialization:  $\sigma_{s,\text{left}}^2 = \sigma_{s,C}^2(\theta)$  as in (33), tolerance  $\epsilon$ 
2: repeat
3:    $\sigma_{s,\text{right}}^2 \leftarrow 2\sigma_{s,\text{left}}^2$ 
4:   Calculate  $\alpha = \left. \frac{dg}{d\sigma_s^2} \right|_{\sigma_{s,\text{right}}^2}$  as given in (37)
5:   if  $\alpha > 0$  then
6:      $\sigma_{s,\text{left}}^2 \leftarrow \sigma_{s,\text{right}}^2$ 
7:   end if
8: until  $\alpha > 0$ 
9: Determine the root  $\sigma_{s,U}^2$  of (37) by bisection search on  $[\sigma_{s,\text{left}}^2, \sigma_{s,\text{right}}^2]$  with the tolerance  $\epsilon$ 
10: return  $F_{\text{PR-UCF}}(\theta) = \frac{1}{\sum_{k=N}^M \lambda_k^2 \left( \hat{\mathbf{R}} - \tilde{\sigma}_{s,U}^2 \mathbf{a}(\theta) \mathbf{a}(\theta)^H \right)}$ 

```

V. COMPUTATIONAL ASPECTS OF THE PARTIAL RELAXATION METHODS

As introduced in Section IV, the proposed partial relaxation approach yields estimation procedures which require extensive eigenvalue computation for the evaluation of the pseudo-spectrum over the entire angle-of-view. In fact, the pseudo-spectra in (26), (28) and (34) and Algorithm 1 depend only on the eigenvalues and therefore the explicit computation of the eigenvectors can be avoided. Generally, if no particular structure of the matrix is exploited, the eigenvalue decomposition requires $O(K^2L)$ operations where K is the dimension of the matrix and L is the number of required eigenvalues [29]. This computational complexity may be prohibitive for specific practical applications and limit the usage of the proposed partial relaxation approach in practice if no acceleration step is considered. Furthermore, from an algorithmic perspective, the expressions in Equation (26), (28), (34) and Algorithm 1 share a common underlying problem structure in the sense that they all require, as a main algorithmic task, the computation of the eigenvalues of a generic matrix form as follows:

$$\mathbf{D} - \rho \mathbf{z} \mathbf{z}^H = \bar{\mathbf{U}} \bar{\mathbf{D}} \bar{\mathbf{U}}^H, \quad (43)$$

where $\mathbf{D} = \text{diag}(d_1, \dots, d_K) \in \mathbb{R}^{K \times K}$ is a constant real diagonal matrix, $\rho \in \mathbb{R}$ is an arbitrary positive real scalar and $\mathbf{z} = [z_1, \dots, z_K]^T \in \mathbb{C}^{K \times 1}$ is a direction-dependent complex-valued vector. The relationship between the generic form in (43) and the pseudo-spectra in (26), (28), (34) and Algorithm 1 is further detailed in the subsections below. Since the expression on the left hand side of (43) denotes a Hermitian matrix obtained by subtracting a rank-one matrix from a constant diagonal matrix,

the term *rank-one modified Hermitian matrix* is adopted. As presented in the following subsections, this particular structure allows a faster implementation of the eigenvalue decomposition, and thus accelerates the computation of the pseudo-spectrum of the partial relaxation methods.

A. Eigenvalue Decomposition of a Rank-One Modified Hermitian Matrix

Initially proposed by Bunch, Nielsen and Sorensen in [30] as a support for calculating the eigenvalues and eigenvectors of symmetric tridiagonal matrices in parallel, the procedure of determining a complex-valued eigensystem of a rank-one modified Hermitian matrix is based on the interlacing theorem as follows [31]:

Theorem 1: Let $\{d_1, \dots, d_K\}$ be the elements on the diagonal of the matrix $\mathbf{D} \in \mathbb{R}^{K \times K}$ where $\{d_1, \dots, d_K\}$ are distinct and sorted in descending order. Further assume that $\rho > 0$ and $\mathbf{z} \in \mathbb{C}^{K \times 1}$ contains only non-zero entries. If the eigenvalues $\{\bar{d}_1, \dots, \bar{d}_K\}$ of the matrix $\mathbf{D} - \rho \mathbf{z} \mathbf{z}^H$ are also sorted in descending order, then:

- $\{\bar{d}_1, \dots, \bar{d}_K\}$ are the K zeros of the secular function $p(x) = 0$, where $p(x)$ is given by:

$$p(x) = 1 - \rho \mathbf{z}^H (\mathbf{D} - x \mathbf{I}_K)^{-1} \mathbf{z} \quad (44)$$

$$= 1 - \rho \sum_{k=1}^K \frac{|\mathbf{z}_k|^2}{d_k - x}. \quad (45)$$

- $\{\bar{d}_1, \dots, \bar{d}_K\}$ satisfy the interlacing property, i.e.,

$$d_1 > \bar{d}_1 > d_2 > \bar{d}_2 > \dots > d_K > \bar{d}_K. \quad (46)$$

- The eigenvector $\bar{\mathbf{u}}_k$ associated with the eigenvalue \bar{d}_k is a multiple of $(\mathbf{D} - \bar{d}_k \mathbf{I}_K)^{-1} \mathbf{z}$

Based on Theorem 1, rooting the secular function in (45) is of great importance for the acceleration of our proposed partial relaxation approach. Due to the structure of the secular function in (45) and the interlacing property in (46), the zeros of the secular function can be determined independently of each other, thus allowing further improvement in computational time through parallel computing. Without loss of generality, assume that the k -th root of the secular function \bar{d}_k which lies inside the interval (d_{k+1}, d_k) where $k = 1, \dots, K$ and $d_{K+1} = -\infty$ is under consideration. By defining the two auxiliary rational functions:

$$\psi_k(x) \triangleq -\rho \sum_{j=1}^k \frac{|\mathbf{z}_j|^2}{d_j - x} \quad (47)$$

$$\phi_k(x) \triangleq \begin{cases} -\rho \sum_{j=k+1}^K \frac{|\mathbf{z}_j|^2}{d_j - x} & \text{if } 1 \leq k \leq K-1 \\ 0 & \text{if } k = K, \end{cases} \quad (48)$$

the secular function in (45) can be rewritten as:

$$-\psi_k(x) = 1 + \phi_k(x). \quad (49)$$

Since both $\psi_k(x)$ and $\phi_k(x)$ are defined as the sum of multiple rational functions, a straightforward approach to solve (49) iteratively from a given point $x^{(\tau)}$ is using rational functions of first degree $\tilde{\psi}_k(x)$ and $\tilde{\phi}_k(x)$, respectively, as approximants. The authors of [30] suggest approximants of type:

$$\tilde{\psi}_k(x) \triangleq \frac{p}{q - x} \quad (50)$$

$$\tilde{\phi}_k(x) \triangleq r + \frac{s}{d_{k+1} - x}, \quad (51)$$

and choose the parameters p, q, r and s such that the approximants coincide at a given point $x^{(\tau)}$ with the corresponding exact functions in (47) and (48), respectively, up to the first derivative. A special case is obtained when $k = K$, in which $\tilde{\phi}_K(x) \triangleq 0$ is chosen. Different choices of the approximants were also introduced and discussed in [32], [33]. For convenience purposes, the steps for determining the roots of the secular function in (45) are summarized in Algorithm 2. Since the approximants in (50) and (51) are rational functions of degree one, the steps in (52)-(56) can be solved in closed form and therefore the complexity for each iteration τ is $O(1)$. As a result, the complexity of the eigenvalue decomposition procedure is $O(KLI)$, where L is the number of required eigenvalues, and I is the number of iterations required for the convergence of Algorithm 2. Note that Algorithm 2 has a quadratic convergence behavior [30], and from simulation results, the number of iteration I required for the accuracy $\epsilon = 10^{-9}$ is less than 6. Therefore, we can assume that the computational complexity of the eigenvalue decomposition using the rational approximation is of order $O(KL)$.

Algorithm 2 Determining the k -th root of the secular function

- 1: **Initialization:** Iteration index $\tau = 0$, $x^{(0)} = d_k - \delta$ where δ is a small constant such that $x^{(0)} > \bar{d}_k$
- 2: **repeat**
- 3: Find the parameter p and q of the rational function $\tilde{\psi}_k(x) = \frac{p}{q-x}$ such that:
$$\tilde{\psi}_k(x^{(\tau)}) = \psi_k(x^{(\tau)}) \quad (52)$$

$$\frac{d\tilde{\psi}_k}{dx} \Big|_{x^{(\tau)}} = \frac{d\psi_k}{dx} \Big|_{x^{(\tau)}} \quad (53)$$
- 4: **if** $k \leq K - 1$ **then**
- 5: Find the parameter r and s of the rational function $\tilde{\phi}_k(x) = r + \frac{s}{d_{k+1} - x}$ such that:
$$\tilde{\phi}_k(x^{(\tau)}) = \phi_k(x^{(\tau)}) \quad (54)$$

$$\frac{d\tilde{\phi}_k}{dx} \Big|_{x^{(\tau)}} = \frac{d\phi_k}{dx} \Big|_{x^{(\tau)}} \quad (55)$$
- 6: **else**
- 7: $\tilde{\phi}_k(x) \equiv 0$
- 8: **end if**
- 9: Find the solution $x^{(\tau+1)} \in (d_{k+1}, d_k)$ of the equation:
$$-\tilde{\psi}_k(x) = 1 + \tilde{\phi}_k(x) \quad (56)$$
- 10: $\tau \leftarrow \tau + 1$
- 11: **until** $|x^{(\tau+1)} - x^{(\tau)}| < \epsilon$
- 12: **return** $\bar{d}_k = x^{(\tau+1)}$

B. Application to PR-DML

As mentioned in Subsection V-A, the complexity of evaluating the pseudo-spectrum is proportional to the number of required eigenvalues L . Therefore, to accelerate the computation of the pseudo-spectrum of the PR-DML method, we reduce the number of required eigenvalues by rewriting the denominator of the expression in (26) as follows:

$$\begin{aligned} \sum_{k=N}^M \lambda_k \left(\mathbf{P}_a^\perp \hat{\mathbf{R}} \right) &= \text{tr} \left\{ \mathbf{P}_a^\perp \hat{\mathbf{R}} \right\} - \sum_{k=1}^{N-1} \lambda_k \left(\mathbf{P}_a^\perp \hat{\mathbf{R}} \right) \\ &= \text{tr} \left\{ \hat{\mathbf{R}} \right\} - \frac{\mathbf{a}^H \hat{\mathbf{R}} \mathbf{a}}{\mathbf{a}^H \mathbf{a}} - \sum_{k=1}^{N-1} \lambda_k \left(\mathbf{P}_a^\perp \hat{\mathbf{R}} \right). \end{aligned} \quad (57)$$

Using the reformulation in (57), only $(N - 1)$ - eigenvalues out of M eigenvalues of $\mathbf{P}_a^\perp \hat{\mathbf{R}}$ are computed and therefore the computational complexity is reduced. In order to apply the eigenvalue decomposition procedure presented in Subsection V-A, the term $\lambda_k \left(\mathbf{P}_a^\perp \hat{\mathbf{R}} \right)$ is further rewritten as follows:

$$\begin{aligned} \lambda_k \left(\mathbf{P}_a^\perp \hat{\mathbf{R}} \right) &= \lambda_k \left(\hat{\mathbf{R}}^{1/2} \mathbf{P}_a^\perp \hat{\mathbf{R}}^{1/2} \right) \\ &= \lambda_k \left(\hat{\mathbf{R}} - \frac{1}{\|\mathbf{a}\|_2^2} \hat{\mathbf{R}}^{1/2} \mathbf{a} \mathbf{a}^H \hat{\mathbf{R}}^{1/2} \right) \\ &= \lambda_k \left(\hat{\Lambda} - \frac{1}{\|\mathbf{a}\|_2^2} \hat{\Lambda}^{1/2} \hat{\mathbf{U}}^H \mathbf{a} \mathbf{a}^H \hat{\mathbf{U}} \hat{\Lambda}^{1/2} \right). \end{aligned} \quad (58)$$

From the expression in (58), the eigenvalue decomposition procedure introduced in Subsection V-A is applied with $\mathbf{D} = \hat{\Lambda}$, $\rho = \frac{1}{\|\mathbf{a}\|_2^2}$ and $\mathbf{z} = \hat{\Lambda}^{1/2} \hat{\mathbf{U}}^H \mathbf{a}$. From the computational perspective, except for the initial full eigenvalue decomposition in (6a), the overall complexity of the calculation of the pseudo-spectrum for the complete angle-of-view with N_G directions is $O((M^2 + M(N - 1)) N_G) = O(M^2 N_G)$. This is higher than the complexity required for computing the MUSIC pseudo-spectrum, which is $O(M N N_G)$.

C. Application to PR-WSF

A similar iterative procedure for computing the eigenvalue decomposition as proposed in Subsection V-A and Subsection V-B can be applied directly to the PR-WSF method presented in Subsection IV-C. However, the computational complexity of the PR-WSF method can be even further reduced due to the fact that all eigenvalues $\lambda_k(\mathbf{P}_a^\perp \hat{\mathbf{U}}_s \mathbf{W} \hat{\mathbf{U}}_s^H)$ with $k = N+1, \dots, M$ are equal to zeros since $\text{rank}(\mathbf{P}_a^\perp \hat{\mathbf{U}}_s \mathbf{W} \hat{\mathbf{U}}_s^H) \leq N$. Therefore, only the N -th eigenvalue $\lambda_N(\mathbf{P}_a^\perp \hat{\mathbf{U}}_s \mathbf{W} \hat{\mathbf{U}}_s^H)$ needs to be calculated. Furthermore, the dimension of the matrix \mathbf{D} in (43) can also be reduced. In fact, similar to (57), it can be shown that:

$$\begin{aligned} & \lambda_N(\mathbf{P}_a^\perp \hat{\mathbf{U}}_s \mathbf{W} \hat{\mathbf{U}}_s^H) \\ &= \lambda_N\left(\mathbf{W} - \frac{1}{\|\mathbf{a}\|_2^2} \mathbf{W}^{1/2} \hat{\mathbf{U}}_s^H \mathbf{a} \mathbf{a}^H \hat{\mathbf{U}}_s \mathbf{W}^{1/2}\right). \end{aligned} \quad (59)$$

Using the identity in (59), the procedure for computing the eigenvalue decomposition introduced in Subsection V-A is applied with $\mathbf{D} = \mathbf{W}$, $\rho = \frac{1}{\|\mathbf{a}\|_2^2}$ and $\mathbf{z} = \mathbf{W}^{1/2} \hat{\mathbf{U}}_s^H \mathbf{a}$. Since the dimension of the matrix is reduced from $M \times M$ to $N \times N$, and only a single eigenvalue is required, the complexity reduces to $O((NM + N - 1)N_G) = O(MNN_G)$, which is identical to the computational complexity of the MUSIC algorithm. However, the computational overhead associated with PR-WSF is still higher than MUSIC since in the preprocessing step of the sample covariance matrix, a full eigenvalue decomposition as in (6b) is required to obtain $\hat{\mathbf{U}}$ and \mathbf{W} .

D. Application to PR-CCF

The expression of the PR-CCF pseudo-spectrum in (34) resembles the generic formulation of the rank-one modified Hermitian matrix in (43), except for the fact that the matrix $\hat{\mathbf{R}}$ is generally not diagonal. Therefore the application of the eigenvalue decomposition in Subsection V-A is trivial by performing an orthogonal transformation on $\hat{\mathbf{R}}$ and \mathbf{a} to diagonalize $\hat{\mathbf{R}}$. However, the number of the eigenvalues required for the computation of the pseudo-spectrum is $M - N + 1$, which is typically larger than the number of sources N . By applying the property of the trace operator, only the $(N - 1)$ -largest eigenvalues are calculated and the inverse of the pseudo-spectrum of the PR-CCF method is rewritten in the following form to utilize the principal eigenvalues:

$$\begin{aligned} \sum_{k=N}^M \lambda_k^2 \left(\hat{\mathbf{R}} - \hat{\sigma}_{s,C}^2 \mathbf{a} \mathbf{a}^H \right) &= \sum_{k=N}^M \lambda_k \left(\left(\hat{\mathbf{R}} - \hat{\sigma}_{s,C}^2 \mathbf{a} \mathbf{a}^H \right)^2 \right) \\ &= \text{tr} \left\{ \left(\hat{\mathbf{R}} - \hat{\sigma}_{s,C}^2 \mathbf{a} \mathbf{a}^H \right)^2 \right\} - \sum_{k=1}^{N-1} \lambda_k^2 \left(\hat{\mathbf{R}} - \hat{\sigma}_{s,C}^2 \mathbf{a} \mathbf{a}^H \right) \\ &= \text{tr} \left\{ \hat{\mathbf{R}}^2 \right\} - 2\hat{\sigma}_{s,C}^2 \mathbf{a}^H \hat{\mathbf{R}} \mathbf{a} + \hat{\sigma}_{s,C}^4 \|\mathbf{a}\|_2^4 \\ &\quad - \sum_{k=1}^{N-1} \lambda_k^2 \left(\hat{\mathbf{R}} - \hat{\sigma}_{s,C}^2 \mathbf{a} \mathbf{a}^H \right). \end{aligned} \quad (60)$$

Considering the formulation in (60), we observe that the PR-CCF method involves both the conventional and Capon beamformer in the calculation of the pseudo-spectrum. Similarly to the PR-DML method, for any eigenvalue $\lambda_k(\hat{\mathbf{R}} - \hat{\sigma}_{s,C}^2 \mathbf{a} \mathbf{a}^H)$, it can be shown that:

$$\lambda_k(\hat{\mathbf{R}} - \hat{\sigma}_{s,C}^2 \mathbf{a} \mathbf{a}^H) = \lambda_k(\hat{\mathbf{\Lambda}} - \hat{\sigma}_{s,C}^2 \hat{\mathbf{U}}^H \mathbf{a} \mathbf{a}^H \hat{\mathbf{U}}). \quad (61)$$

From (60) and (61), we apply the eigenvalue decomposition procedure presented in Subsection V-A with $\mathbf{D} = \hat{\mathbf{\Lambda}}$, $\rho = \hat{\sigma}_{s,C}^2$ and $\mathbf{z} = \hat{\mathbf{U}}^H \mathbf{a}$ and thus the overall computational complexity of the PR-CCF algorithm is $O((2M^2 + M(N - 1))N_G) = O(M^2N_G)$.

E. Application to PR-UCF

Unlike the PR-DML, PR-WSF and PR-CCF methods, the PR-UCF estimator requires additional steps in calculating the derivative to obtain the minimizer $\sigma_{s,U}^2$ of (36). To reduce the number of required eigenvalues for the derivative, the function $g(\sigma_s^2) = \sum_{k=N}^M \lambda_k^2 \left(\hat{\mathbf{R}} - \sigma_s^2 \mathbf{a} \mathbf{a}^H \right)$ is rewritten similarly to (60) as follows:

$$\begin{aligned} g(\sigma_s^2) &= \text{tr} \left\{ \hat{\mathbf{R}}^2 \right\} - 2\hat{\sigma}_s^2 \mathbf{a}^H \hat{\mathbf{R}} \mathbf{a} + \hat{\sigma}_s^4 \|\mathbf{a}\|_2^4 \\ &\quad - \sum_{k=1}^{N-1} \lambda_k^2 \left(\hat{\mathbf{R}} - \hat{\sigma}_s^2 \mathbf{a} \mathbf{a}^H \right). \end{aligned} \quad (62)$$

The derivative $\frac{dg}{d\sigma_s^2} \Big|_{\sigma_{s,0}^2}$ is calculated as:

$$\begin{aligned} \frac{dg}{d\sigma_s^2} \Big|_{\sigma_{s,0}^2} &= -2\mathbf{a}^H \hat{\mathbf{R}}\mathbf{a} + 2\sigma_{s,0}^2 \|\mathbf{a}\|_2^4 \\ &+ \sum_{k=1}^{N-1} \frac{2\bar{\lambda}_k(\sigma_{s,0}^2)}{\sigma_{s,0}^4 \mathbf{a}^H (\hat{\mathbf{R}} - \bar{\lambda}_k(\sigma_{s,0}^2) \mathbf{I}_M)^{-2} \mathbf{a}} \end{aligned} \quad (63)$$

where $\bar{\lambda}_k(\sigma_{s,0}^2) = \lambda_k(\hat{\mathbf{R}} - \sigma_{s,0}^2 \mathbf{a} \mathbf{a}^H)$. By substituting $\mathbf{z} = \hat{\mathbf{U}}^H \mathbf{a}$, we obtain:

$$\bar{\lambda}_k(\sigma_{s,0}^2) = \lambda_k(\hat{\mathbf{A}} - \sigma_{s,0}^2 \mathbf{z} \mathbf{z}^H) \quad (64)$$

$$\begin{aligned} \frac{dg}{d\sigma_s^2} \Big|_{\sigma_{s,0}^2} &= -2\mathbf{z}^H \hat{\mathbf{A}}\mathbf{z} + 2\sigma_{s,0}^2 \|\mathbf{z}\|_2^4 \\ &+ \sum_{k=1}^{N-1} \frac{2\bar{\lambda}_k(\sigma_{s,0}^2)}{\sigma_{s,0}^4 \sum_{j=1}^M \frac{|\mathbf{z}_j|^2}{(\hat{\lambda}_j - \bar{\lambda}_k(\sigma_{s,0}^2))^2}}. \end{aligned} \quad (65)$$

The expressions in (64) and (65) suggest to apply the procedure in Subsection V-A with $\mathbf{D} = \hat{\mathbf{A}}$, $\rho = \sigma_{s,0}^2$ and $\mathbf{z} = \hat{\mathbf{U}}^H \mathbf{a}$. The computational complexity of the PR-UCF method is therefore of order $O(M^2 N_G N_I)$ where N_I is the number of bisection steps conducted in Algorithm 1.

VI. SIMULATION RESULTS

In this section, simulation results regarding the performance of different DOA estimators are presented and compared with the stochastic Cramer-Rao Bound (CRB) [7]. The number of Monte-Carlo runs is 1000. The key performance indicators are the Root-Mean-Squared-Error (RMSE), which is calculated as:

$$\text{RMSE} = \sqrt{\frac{\sum_{n=1}^N (\tilde{\theta}_n - \theta_n)^2}{N}}, \quad (66)$$

and the execution time for each Monte-Carlo run. The estimated DOAs $\tilde{\boldsymbol{\theta}} = [\tilde{\theta}_1, \dots, \tilde{\theta}_N]^T$ and the true DOAs $\boldsymbol{\theta} = [\theta_1, \dots, \theta_N]^T$ in (66) are sorted in ascending order. The simulation is conducted in MATLAB 2016b on a PC equipped with an OS of Arch Linux with a processor 8 x Intel Core i7-6700 4.00GHz CPU and 16GB RAM. The iterative eigenvalue decomposition introduced in Subsection V-A is implemented in C and imported in MATLAB through a MEX interface. In our simulations we assume, if not further specified, two uncorrelated but closely spaced source signals at $\boldsymbol{\theta} = [45^\circ, 50^\circ]^T$ which impinge on a ULA of $M = 10$ antennas with the spacing equal to half of the wavelength. The source signals have the mean value of zero and unit power. The Signal-to-Noise-Ratio (SNR) is calculated as $\text{SNR} = \frac{1}{\sigma_n^2}$. Regarding the PR-WSF method, we choose the weighting as in (14). As depicted in Figure 1, the partial relaxation methods exhibit a superior SNR threshold performance in comparison to the MUSIC algorithm. The PR-CCF and PR-UCF estimator possess almost identical estimation error performance in the inspected SNR region where their threshold occurs at an even lower SNR than root-MUSIC. This remark suggests that PR-CCF is more favorable in this regime than PR-UCF since the theoretical computational complexity of PR-CCF is lower than that of PR-UCF while the error performances are comparable. Both the RMSE of PR-CCF and PR-UCF do not approach the CRB. PR-DML and PR-WSF have similar performance behaviors, achieving the CRB at a lower SNR than MUSIC.

In the next simulation, we consider the signals of two correlated sources. The correlation coefficient ρ is defined as:

$$\rho = \frac{\mathbb{E} \{ s_1(t)^H s_2(t) \}}{\sqrt{\mathbb{E} \{ |s_1(t)|^2 \} \mathbb{E} \{ |s_2(t)|^2 \}}}. \quad (67)$$

In Figure 2, the correlation coefficient is set to $\rho = 0.95$. The number of snapshots is increased to $T = 200$. Note that spatial smoothing is not applied. The threshold of root-MUSIC now occurs at a lower SNR than the partial relaxation methods. However, in the post-threshold region, all estimators in the partial relaxation family have a lower RMSE than root-MUSIC.

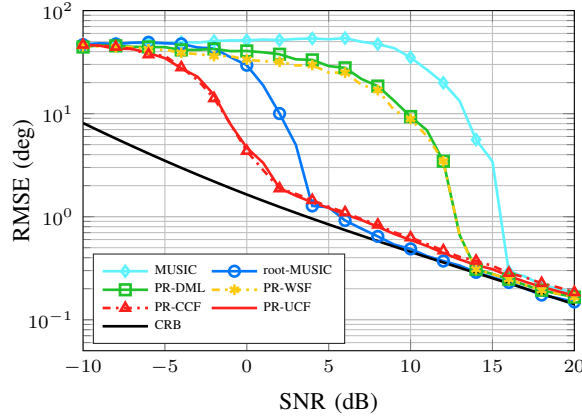


Figure 1: Uncorrelated source signal, number of snapshots $T = 40$

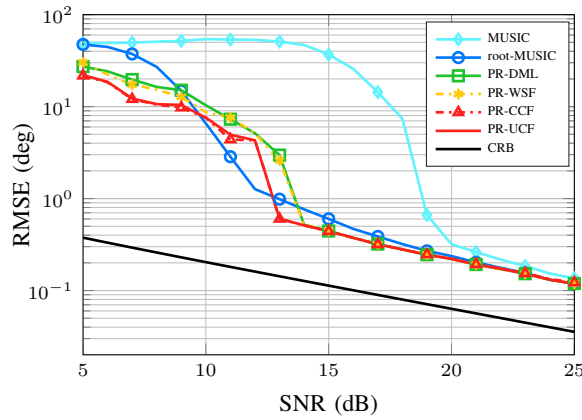


Figure 2: Correlated sources with $\rho = 0.95$, number of snapshots $T = 200$

In the next simulation, as depicted in Figure 3, SNR is fixed at 3 dB, and the number of snapshots T is varied between 10 and 10000. Again the PR-CCF and PR-UCF estimator possess the best threshold performance at $T = 30$ samples. However, in the post-threshold region, the RMSE of PR-CCF and PR-UCF is not as close to the CRB as root-MUSIC and PR-DML. PR-WSF outperforms PR-DML consistently in this simulation. In general, the partial relaxation methods outperform MUSIC.

In the fourth setup, the first source is fixed at $\theta_1 = 45^\circ$ and the angular separation between two sources $\Delta\theta$ is varied from 0.5° to 6° . In Figure 4, the RMSE of PR-CCF/PR-UCF is close to the Cramer-Rao Bound even when the angular separation $\Delta\theta$ is as small as 1.25° . However, the RMSE of PR-CCF/PR-UCF slowly achieves the CRB only when $\Delta\theta > 5^\circ$. PR-WSF slightly outperforms PR-DML, and both algorithms outperform MUSIC.

Figure 5 depicts a scenario where the number of snapshots $T = 8$ is smaller than the number of antennas $M = 10$. In this case, the sample covariance matrix calculated in (5) is singular, and therefore the PR-CCF is not applicable. In this case, we apply the diagonal loading technique with the loading factor $\gamma = 10^{-4}$ on the sample covariance matrix [34], [25]. The initialization for $\sigma_{s,\text{left}}^2$ of Algorithm 1 is set at $\sigma_{s,\text{left}}^2 = 10^{-6}$. To avoid outliers in RMSE caused by misdetection and to simulate the DOA tracking process [35], 1% of the estimates with the largest error for all investigated algorithms are removed before calculating the RMSE. It can be observed that even in the case of a very low number of snapshots, PR-UCF obtains the best SNR threshold behavior. However, the RMSE of PR-UCF only slowly approaches the Cramer-Rao Bound as the SNR increases. The performance of PR-CCF is highly degraded due to the diagonal loading. Further research may be carried out regarding the optimal adaptive choice of the diagonal loading factor γ to achieve an improved performance using a direction-dependent factor. However, this is beyond the scope of this paper and therefore left for further research. Similar to the above-investigated scenarios, PR-DML and PR-WSF outperform MUSIC consistently.

In Figure 6, the execution time of the DOA estimation algorithms with respect to the number of antennas M are depicted. The angle-of-view is partitioned uniformly into $N_G = 1800$ directions. The term *Generic* in Figure 6 refers to the naive implementation using the MATLAB command `eig` for the eigenvalue decomposition. The polynomial rooting applied for root-

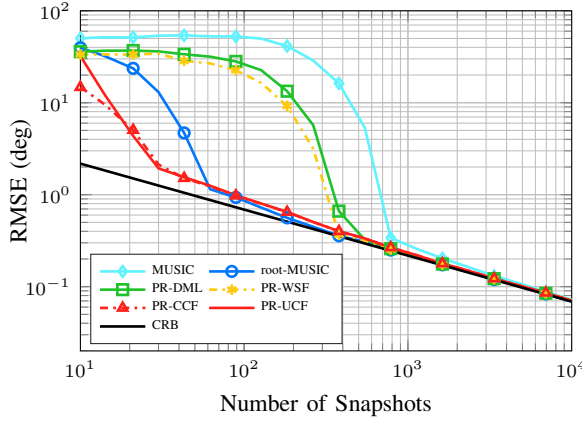


Figure 3: Uncorrelated source signal, SNR = 3 dB

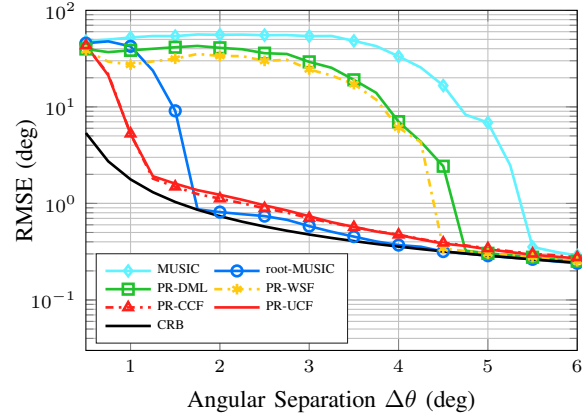
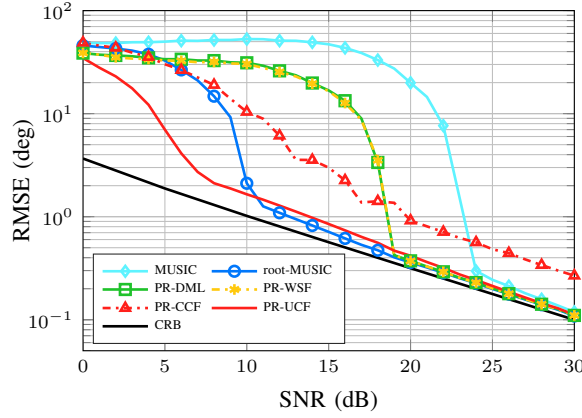
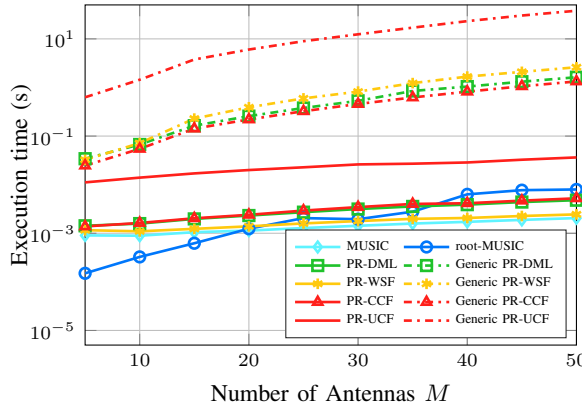


Figure 4: Uncorrelated source signal, SNR = 10 dB, number of snapshots $T = 100$

MUSIC relies on determining the eigenvalues of the companion matrix and therefore the execution time increases drastically with respect to the number of antennas M . All partial relaxation methods except for PR-UCF follow similar trends as MUSIC where the execution time is in the same order of magnitude. The execution time of the PR-UCF estimator is approximately ten times larger than other partial relaxation methods. Nevertheless, the PR-UCF estimator based on the efficient eigenvalue decomposition introduced in Section V requires less execution time than the direct implementation with the MATLAB command. Generally, thanks to the quadratic convergence behavior of Algorithm 2, the execution time is reduced by a factor of 20 to 1000 in comparison with the direct implementation using the generic command `eig`. PR-WSF even exhibits almost identical execution time behavior as MUSIC, indicating the possibility of applying the partial relaxation methods in practical cases to obtain the excellent threshold performance in the low SNR region.

VII. CONCLUSIONS AND OUTLOOK

In this paper, new DOA estimators using the partial relaxation approach are introduced. Instead of enforcing the full structure on the steering matrix while formulating the DOA estimation problem, in the partial relaxation approach, only the structure in the steering vector of one source of interest is preserved, while the structure of the remaining interfering sources is relaxed. Simulation results show that, even though no particular structure of the sensor array, e.g., Vandermonde structure from a uniform linear array, is required, the methods in the partial relaxation framework, especially the estimator based on the covariance fitting problems, exhibit comparable RMSE performance as root-MUSIC and superior to spectral MUSIC in difficult scenarios. In comparison with the unconstrained covariance fitting estimator, the inner approximation in the constrained variant helps to reduce the computational complexity without necessarily sacrificing the error performance. By applying known results regarding rank-one modifications of a Hermitian matrix, the pseudo-spectra of the partial relaxation methods are efficiently calculated. Our simulation results reveal that among the methods in the partial relaxation family, Weighted Subspace Fitting and the constrained covariance fitting variant are preferable to Deterministic Maximum Likelihood and the unconstrained covariance fitting counterparts, respectively, in non-degenerate cases due to comparable resolution capability but considerably lower computational time.

Figure 5: Uncorrelated source signal, number of snapshots $T = 8$ Figure 6: SNR = 10 dB, number of snapshots $T = 100$

For future work, the theoretical error behavior and consistency of methods in the family of the partial relaxation approach is an interesting open problem and requires further investigation.

APPENDIX A PROOF OF (25)

In order to prove the identity in (25), we first introduce two important prepositions:

Proposition 1: Let $\mathbf{B} \in \mathbb{C}^{M \times (N-1)}$ be a non-zero matrix and $\mathbf{a} \in \mathbb{C}^{M \times 1}$ be a non-zero vector such that $\mathbf{P}_{\mathbf{a}}^{\perp} \mathbf{B}$ is a non-zero matrix. Then there always exists a matrix $\mathbf{Z} \in \mathbb{C}^{M \times N'}$ with $1 \leq N' \leq N-1$ such that the following conditions are satisfied:

$$\mathbf{P}_{\mathbf{P}_{\mathbf{a}}^{\perp} \mathbf{B}} = \mathbf{Z} \mathbf{Z}^H \quad (68a)$$

$$\mathbf{Z}^H \mathbf{Z} = \mathbf{I}_{N'} \quad (68b)$$

$$\mathbf{Z}^H \mathbf{a} = \mathbf{0}. \quad (68c)$$

Proof of Proposition 1: First expand $\mathbf{P}_{\mathbf{P}_{\mathbf{a}}^{\perp} \mathbf{B}}$ in the following manner:

$$\begin{aligned} \mathbf{P}_{\mathbf{P}_{\mathbf{a}}^{\perp} \mathbf{B}} &= \mathbf{P}_{\mathbf{a}}^{\perp} \mathbf{B} \left(\left(\mathbf{P}_{\mathbf{a}}^{\perp} \mathbf{B} \right)^H \left(\mathbf{P}_{\mathbf{a}}^{\perp} \mathbf{B} \right) \right)^{-1} \left(\mathbf{P}_{\mathbf{a}}^{\perp} \mathbf{B} \right)^H \\ &= \mathbf{P}_{\mathbf{a}}^{\perp} \mathbf{B} \left(\mathbf{B}^H \mathbf{P}_{\mathbf{a}}^{\perp} \mathbf{B} \right)^{-1} \mathbf{B}^H \mathbf{P}_{\mathbf{a}}^{\perp}. \end{aligned} \quad (69)$$

The rank of the matrix $\mathbf{P}_{\mathbf{P}_{\mathbf{a}}^{\perp} \mathbf{B}}$ can therefore be bounded by:

$$\begin{aligned} 1 \leq N' &= \text{rank} \left(\mathbf{P}_{\mathbf{P}_{\mathbf{a}}^{\perp} \mathbf{B}} \right) \\ &\leq \min \left\{ \text{rank} \left(\mathbf{P}_{\mathbf{a}}^{\perp} \right), \text{rank} \left(\mathbf{B} \right), \text{rank} \left(\left(\mathbf{B}^H \mathbf{P}_{\mathbf{a}}^{\perp} \mathbf{B} \right) \right) \right\} \\ &\leq N-1 \end{aligned} \quad (70)$$

Furthermore, since $\mathbf{P}_{\mathbf{P}_a^\perp \mathbf{B}}$ contains only the eigenvalues 0 and 1, taking the eigenvalue decomposition of $\mathbf{P}_{\mathbf{P}_a^\perp \mathbf{B}}$ yields:

$$\mathbf{P}_{\mathbf{P}_a^\perp \mathbf{B}} = \mathbf{Z} \mathbf{Z}^H, \quad (71)$$

and the number of columns of \mathbf{Z} is equal to N' . Clearly the matrix $\mathbf{Z} \in \mathbb{C}^{M \times N'}$ satisfies $\mathbf{Z}^H \mathbf{Z} = \mathbf{I}_{N'}$. Therefore, conditions in (68a) and (68b) are satisfied if \mathbf{Z} is chosen as in (71). Finally, we further observe that:

$$\begin{aligned} \mathbf{a}^H \mathbf{Z} \mathbf{Z}^H \mathbf{a} &= \mathbf{a}^H \mathbf{P}_{\mathbf{P}_a^\perp \mathbf{B}} \mathbf{a} \\ &= \mathbf{a}^H \mathbf{P}_a^\perp \mathbf{B} \left(\mathbf{B}^H \mathbf{P}_a^\perp \mathbf{B} \right)^{-1} \mathbf{B}^H \mathbf{P}_a^\perp \mathbf{a} = 0 \end{aligned} \quad (72)$$

The identity in (68c) follows immediately from (72). \blacksquare

Proposition 2: Let $\mathbf{a} \in \mathbb{C}^{M \times 1}$ be a non-zero vector and $\hat{\mathbf{R}} \in \mathbb{C}^{M \times M}$ be a non-zero Hermitian positive semidefinite matrix. Then the eigenvectors which correspond to non-zero eigenvalues of $\mathbf{P}_a^\perp \hat{\mathbf{R}} \mathbf{P}_a^\perp$ are orthogonal to \mathbf{a} .

Proof of Proposition 2: Let \mathbf{x} be an eigenvector corresponding to an eigenvalue $\lambda \neq 0$ of $\mathbf{P}_a^\perp \hat{\mathbf{R}} \mathbf{P}_a^\perp$, then by definition:

$$\mathbf{P}_a^\perp \hat{\mathbf{R}} \mathbf{P}_a^\perp \mathbf{x} = \lambda \mathbf{x}. \quad (73)$$

Taking the conjugate transpose of (73) and multiplying with \mathbf{a} on the right, we obtain:

$$0 = \mathbf{x}^H \mathbf{P}_a^\perp \hat{\mathbf{R}} \mathbf{P}_a^\perp \mathbf{a} = \left(\mathbf{P}_a^\perp \hat{\mathbf{R}} \mathbf{P}_a^\perp \mathbf{x} \right)^* \mathbf{a} = \lambda^* \mathbf{x}^H \mathbf{a}. \quad (74)$$

From (74) and the assumption that λ is non-zero, we can conclude that \mathbf{x} is orthogonal to \mathbf{a} . \blacksquare

Now we return to the main proof of (25). In the case that $\mathbf{P}_a^\perp \mathbf{B} = \mathbf{0}$, then by convention in Subsection IV-B, we obtain that $\text{tr} \{ \mathbf{P}_{\mathbf{P}_a^\perp \mathbf{B}} \hat{\mathbf{R}} \} = 0$. On the other hand, if the matrix $\mathbf{P}_a^\perp \mathbf{B}$ is a non-zero matrix, applying the decomposition (68) in Proposition 1 and considering that $\mathbf{Z}^H \mathbf{a} = 0$, the objective function in (25) is rewritten as follows:

$$\begin{aligned} \text{tr} \{ \mathbf{P}_{\mathbf{P}_a^\perp \mathbf{B}} \hat{\mathbf{R}} \} &= \text{tr} \{ \mathbf{Z} \mathbf{Z}^H \hat{\mathbf{R}} \} = \text{tr} \{ \mathbf{Z}^H \hat{\mathbf{R}} \mathbf{Z} \} \\ &= \text{tr} \{ \mathbf{Z}^H \left(\mathbf{P}_a + \mathbf{P}_a^\perp \right) \hat{\mathbf{R}} \left(\mathbf{P}_a + \mathbf{P}_a^\perp \right) \mathbf{Z} \} \\ &= \text{tr} \{ \mathbf{Z}^H \mathbf{P}_a^\perp \hat{\mathbf{R}} \mathbf{P}_a^\perp \mathbf{Z} \}. \end{aligned} \quad (75)$$

Therefore the optimization problem in (25) is reformulated as:

$$\underset{\mathbf{Z}}{\text{maximize}} \text{tr} \{ \mathbf{Z}^H \mathbf{P}_a^\perp \hat{\mathbf{R}} \mathbf{P}_a^\perp \mathbf{Z} \} \quad (76a)$$

$$\text{subject to } \mathbf{Z} \in \mathbb{C}^{M \times N'} \quad (76b)$$

$$\mathbf{Z}^H \mathbf{Z} = \mathbf{I}_{N'} \quad (76c)$$

$$\mathbf{Z}^H \mathbf{a} = \mathbf{0}. \quad (76d)$$

Relaxing the constraint $\mathbf{Z}^H \mathbf{a} = 0$ in (76d), from the Ky-Fan inequality in [36], the optimization in (76) admits a maximizer $\tilde{\mathbf{Z}}$ whose columns form an orthonormal basis of the eigenspace associated with the N' -largest eigenvalues of $\mathbf{P}_a^\perp \hat{\mathbf{R}} \mathbf{P}_a^\perp$. However, from Proposition 2, the eigenvectors associated with non-zero eigenvalues of $\mathbf{P}_a^\perp \hat{\mathbf{R}} \mathbf{P}_a^\perp$ are orthogonal to \mathbf{a} . Therefore, the relaxation of the constraint in (76d) does not affect the maximizer $\tilde{\mathbf{Z}}$ of the optimization problem in (76). As a consequence, we obtain the following result:

$$\begin{aligned} \sum_{k=1}^{N'} \lambda_k \left(\mathbf{P}_a^\perp \hat{\mathbf{R}} \mathbf{P}_a^\perp \right) &= \max \text{tr} \{ \mathbf{Z}^H \mathbf{P}_a^\perp \hat{\mathbf{R}} \mathbf{P}_a^\perp \mathbf{Z} \} \\ \text{subject to } \mathbf{Z} &\in \mathbb{C}^{M \times N'} \end{aligned} \quad (77)$$

$$\mathbf{Z}^H \mathbf{Z} = \mathbf{I}_{N'},$$

$$\mathbf{Z}^H \mathbf{a} = \mathbf{0}.$$

Combining (70), (75) and (77), the following identity is obtained:

$$\begin{aligned} \max_{\mathbf{B} \in \mathbb{C}^{M \times (N-1)}} \text{tr} \{ \mathbf{P}_{\mathbf{P}_a^\perp \mathbf{B}} \hat{\mathbf{R}} \} &= \sum_{k=1}^{N-1} \lambda_k \left(\mathbf{P}_a^\perp \hat{\mathbf{R}} \mathbf{P}_a^\perp \right) \\ &= \sum_{k=1}^{N-1} \lambda_k \left(\mathbf{P}_a^\perp \hat{\mathbf{R}} \right). \end{aligned} \quad (78)$$

The optimum in (78) is achieved if we choose one matrix $\mathbf{B} \in \mathbb{C}^{M \times (N-1)}$ such that $\mathbf{P}_{\mathbf{P}_a^\perp \mathbf{B}} = \mathbf{Z} \mathbf{Z}^H$ and the columns of \mathbf{Z} form an orthonormal basis of the eigenspace associated with non-zero eigenvalues of $\mathbf{P}_a^\perp \hat{\mathbf{R}} \mathbf{P}_a^\perp$

APPENDIX B
EQUIVALENCE OF MUSIC AND PR-WSF WITH $\mathbf{W} = \mathbf{I}_M$

Considering the expression in (28) for the steering vector $\mathbf{a} = \mathbf{a}(\theta)$, we note that the rank of $\mathbf{P}_{\mathbf{a}}^{\perp} \hat{\mathbf{U}}_s \hat{\mathbf{U}}_s^H$ is at most N . Hence, $\lambda_k \left(\mathbf{P}_{\mathbf{a}}^{\perp} \hat{\mathbf{U}}_s \hat{\mathbf{U}}_s^H \right) = 0$ for $k = N + 1, \dots, M$. Therefore, when calculating the pseudo-spectrum in (28), only $\lambda_N \left(\mathbf{P}_{\mathbf{a}}^{\perp} \hat{\mathbf{U}}_s \hat{\mathbf{U}}_s^H \right)$ is considered. The expression for $\lambda_N \left(\mathbf{P}_{\mathbf{a}}^{\perp} \hat{\mathbf{U}}_s \hat{\mathbf{U}}_s^H \right)$ can be further rewritten as follows:

$$\begin{aligned} \lambda_N \left(\mathbf{P}_{\mathbf{a}}^{\perp} \hat{\mathbf{U}}_s \hat{\mathbf{U}}_s^H \right) &= \lambda_N \left(\hat{\mathbf{U}}_s^H \left(\mathbf{I}_M - \frac{1}{\|\mathbf{a}\|_2^2} \mathbf{a} \mathbf{a}^H \right) \hat{\mathbf{U}}_s \right) \\ &= \lambda_N \left(\mathbf{I}_M - \frac{1}{\|\mathbf{a}\|_2^2} \hat{\mathbf{U}}_s^H \mathbf{a} \mathbf{a}^H \hat{\mathbf{U}}_s \right) \\ &= 1 + \lambda_N \left(-\frac{1}{\|\mathbf{a}\|_2^2} \hat{\mathbf{U}}_s^H \mathbf{a} \mathbf{a}^H \hat{\mathbf{U}}_s \right). \end{aligned} \quad (79)$$

Since $-\frac{1}{\|\mathbf{a}\|_2^2} \hat{\mathbf{U}}_s^H \mathbf{a} \mathbf{a}^H \hat{\mathbf{U}}_s$ is a rank-one matrix of size $N \times N$, it can be easily shown that:

$$\lambda_N \left(-\frac{1}{\|\mathbf{a}\|_2^2} \hat{\mathbf{U}}_s^H \mathbf{a} \mathbf{a}^H \hat{\mathbf{U}}_s \right) = -\frac{1}{\|\mathbf{a}\|_2^2} \mathbf{a}^H \hat{\mathbf{U}}_s \hat{\mathbf{U}}_s^H \mathbf{a}. \quad (80)$$

Substituting (80) into (79) and using the orthogonality property between the signal and the noise subspace, we obtain:

$$\begin{aligned} \lambda_N \left(\mathbf{P}_{\mathbf{a}}^{\perp} \hat{\mathbf{U}}_s \hat{\mathbf{U}}_s^H \right) &= 1 - \frac{1}{\|\mathbf{a}\|_2^2} \mathbf{a}^H \left(\mathbf{I}_M - \hat{\mathbf{U}}_n \hat{\mathbf{U}}_n^H \right) \mathbf{a} \\ &= \frac{\mathbf{a}^H \hat{\mathbf{U}}_n \hat{\mathbf{U}}_n^H \mathbf{a}}{\mathbf{a}^H \mathbf{a}}. \end{aligned} \quad (81)$$

The expression in (81) is identical to the null-spectrum of MUSIC. Therefore, with $\mathbf{W} = \mathbf{I}_M$, the expression in (27) is another equivalent formulation of the MUSIC estimator.

APPENDIX C
PROOF OF (33)

Since $\hat{\mathbf{R}} - \hat{\sigma}_{s,C}^2 \mathbf{a} \mathbf{a}^H$ has at least one eigenvalue equal to zero and assuming that $\hat{\mathbf{R}}$ is invertible, we obtain:

$$0 = \det \left(\hat{\mathbf{R}}^{-1} \right) \det \left(\hat{\mathbf{R}} - \hat{\sigma}_{s,C}^2 \mathbf{a} \mathbf{a}^H \right) \quad (82a)$$

$$= \det \left(\mathbf{I}_M - \hat{\mathbf{R}}^{-1} \hat{\sigma}_{s,C}^2 \mathbf{a} \mathbf{a}^H \right) \quad (82b)$$

$$= 1 - \hat{\sigma}_{s,C}^2 \mathbf{a}^H \hat{\mathbf{R}}^{-1} \mathbf{a}, \quad (82c)$$

where the identity $\det(\mathbf{I} + \mathbf{AB}) = \det(\mathbf{I} + \mathbf{BA})$ is applied in (82b)-(82c). From (82c) and solving for $\hat{\sigma}_{s,C}^2$ concludes our proof.

APPENDIX D
PROOF OF (37)

First, by taking the eigenvalue decomposition as in (6b) and substituting $\mathbf{z} = \hat{\mathbf{U}}^H \mathbf{a}$, the inner objective function of the PR-UCF in (36) is rewritten as:

$$g(\sigma_s^2) = \sum_{k=N}^M \lambda_k^2 \left(\hat{\Lambda} - \sigma_s^2 \mathbf{z} \mathbf{z}^H \right). \quad (83)$$

In the following steps, we calculate the derivative $\frac{d\lambda_k \left(\hat{\Lambda} - \sigma_s^2 \mathbf{z} \mathbf{z}^H \right)}{d\sigma_s^2} \Big|_{\sigma_{s,0}^2}$. Applying the results from [37] on the Hermitian matrix $\hat{\Lambda} - \sigma_s^2 \mathbf{z} \mathbf{z}^H$ leads to the following expression:

$$\frac{d\lambda_k \left(\hat{\Lambda} - \sigma_s^2 \mathbf{z} \mathbf{z}^H \right)}{d\sigma_s^2} \Big|_{\sigma_{s,0}^2} = \frac{\bar{\mathbf{u}}_k^H \frac{d \left(\hat{\Lambda} - \sigma_s^2 \mathbf{z} \mathbf{z}^H \right)}{d\sigma_s^2} \Big|_{\sigma_{s,0}^2} \bar{\mathbf{u}}_k}{\bar{\mathbf{u}}_k^H \bar{\mathbf{u}}_k} \quad (84a)$$

$$= -\frac{\bar{\mathbf{u}}_k^H \mathbf{z} \mathbf{z}^H \bar{\mathbf{u}}_k}{\bar{\mathbf{u}}_k^H \bar{\mathbf{u}}_k}, \quad (84b)$$

where $\bar{\mathbf{u}}_k$ is an eigenvector corresponding to the eigenvalue $\lambda_k(\hat{\mathbf{\Lambda}} - \sigma_s^2 \mathbf{z} \mathbf{z}^H)$. Interestingly, the expression on the numerator of (84b) can be shown to be independent of the eigenvectors. In fact, by using the shorthand notation $\bar{\lambda}_k(\sigma_{s,0}^2) = \lambda_k(\hat{\mathbf{\Lambda}} - \sigma_{s,0}^2 \mathbf{z} \mathbf{z}^H)$ as in (38) and applying Property 1 and Property 3 from Theorem 1 to the matrix $\hat{\mathbf{\Lambda}} - \sigma_{s,0}^2 \mathbf{z} \mathbf{z}^H$, we obtain:

$$0 = 1 - \sigma_{s,0}^2 \mathbf{z}^H (\hat{\mathbf{\Lambda}} - \bar{\lambda}_k(\sigma_{s,0}^2) \mathbf{I}_M)^{-1} \mathbf{z} \quad (85)$$

$$\bar{\mathbf{u}}_k = (\hat{\mathbf{\Lambda}} - \bar{\lambda}_k(\sigma_{s,0}^2) \mathbf{I}_M)^{-1} \mathbf{z}. \quad (86)$$

Substituting (85) and (86) into (84b), the derivative of $\lambda_k(\hat{\mathbf{\Lambda}} - \sigma_s^2 \mathbf{z} \mathbf{z}^H)$ with respect to σ_s^2 is given by:

$$\begin{aligned} \frac{d\lambda_k(\hat{\mathbf{\Lambda}} - \sigma_s^2 \mathbf{z} \mathbf{z}^H)}{d\sigma_s^2} \Bigg|_{\sigma_{s,0}^2} &= -\frac{\bar{\mathbf{u}}_k^H \mathbf{z} \mathbf{z}^H \bar{\mathbf{u}}_k}{\bar{\mathbf{u}}_k^H \bar{\mathbf{u}}_k} \\ &= -\frac{\mathbf{z}^H (\hat{\mathbf{\Lambda}} - \bar{\lambda}_k(\sigma_{s,0}^2) \mathbf{I}_M)^{-1} \mathbf{z} \mathbf{z}^H (\hat{\mathbf{\Lambda}} - \bar{\lambda}_k(\sigma_{s,0}^2) \mathbf{I}_M)^{-1} \mathbf{z}}{\mathbf{z}^H (\hat{\mathbf{\Lambda}} - \bar{\lambda}_k(\sigma_{s,0}^2) \mathbf{I}_M)^{-2} \mathbf{z}} \\ &= -\frac{1}{\sigma_{s,0}^4 \mathbf{z}^H (\hat{\mathbf{\Lambda}} - \bar{\lambda}_k(\sigma_{s,0}^2) \mathbf{I}_M)^{-2} \mathbf{z}} \\ &= -\frac{1}{\sigma_{s,0}^4 \mathbf{a}^H (\hat{\mathbf{R}} - \bar{\lambda}_k(\sigma_{s,0}^2) \mathbf{I}_M)^{-2} \mathbf{a}}. \end{aligned} \quad (87)$$

Taking the derivative of (83) by applying the identity in (87) concludes our proof of (37).

REFERENCES

- [1] A. Rembovsky, A. Ashikhmin, V. Kozmin, and S. Smolskiy, *Radio Monitoring: Problems, Methods and Equipment*, ser. Lecture Notes in Electrical Engineering. Springer, 2009.
- [2] H. Van Trees, *Detection, Estimation, and Modulation Theory. Optimum Array Processing*, ser. Detection, Estimation, and Modulation Theory. Wiley, 2004.
- [3] H. Krim and M. Viberg, "Two Decades of Array Signal Processing Research: The Parametric Approach," *Signal Processing Magazine, IEEE*, vol. 13, no. 4, pp. 67–94, Jul 1996.
- [4] P.-J. Chung, M. Viberg, and J. Yu, "Chapter 14 - DOA Estimation Methods and Algorithms," in *Volume 3: Array and Statistical Signal Processing*, ser. Academic Press Library in Signal Processing, R. C. Abdelhak M. Zoubir, Mats Viberg and S. Theodoridis, Eds. Elsevier, 2014, vol. 3, pp. 599 – 650. [Online]. Available: <http://www.sciencedirect.com/science/article/pii/B978012411597200014X>
- [5] P. Stoica and A. Nehorai, "MUSIC, Maximum Likelihood, and Cramer-Rao bound," *IEEE Transactions on Acoustics, Speech, and Signal Processing*, vol. 37, no. 5, pp. 720–741, May 1989.
- [6] P. Stoica and K. C. Sharman, "Maximum Likelihood Methods for Direction-of-Arrival Estimation," *IEEE Transactions on Acoustics, Speech, and Signal Processing*, vol. 38, no. 7, pp. 1132–1143, Jul 1990.
- [7] P. Stoica and A. Nehorai, "Performance Study of Conditional and Unconditional Direction-of-Arrival Estimation," *IEEE Transactions on Acoustics, Speech, and Signal Processing*, vol. 38, no. 10, pp. 1783–1795, Oct 1990.
- [8] R. Schmidt, "Multiple Emitter Location and Signal Parameter Estimation," *Antennas and Propagation, IEEE Transactions on*, vol. 34, no. 3, pp. 276–280, Mar 1986.
- [9] A. Barabell, "Improving the Resolution Performance of Eigenstructure-based Direction-Finding Algorithms," in *Acoustics, Speech, and Signal Processing, IEEE International Conference on ICASSP '83*, vol. 8, Apr 1983, pp. 336–339.
- [10] R. Roy and T. Kailath, "ESPRIT-Estimation of Signal Parameters via Rotational Invariance Techniques," *Acoustics, Speech and Signal Processing, IEEE Transactions on*, vol. 37, no. 7, pp. 984–995, Jul 1989.
- [11] M. Pesavento, A. B. Gershman, and M. Haardt, "Unitary Root-MUSIC With a Real-Valued Eigendecomposition: A Theoretical and Experimental Performance Study," *IEEE Transactions on Signal Processing*, vol. 48, no. 5, pp. 1306–1314, May 2000.
- [12] M. Haardt and J. A. Nossek, "Unitary ESPRIT: How to Obtain Increased Estimation Accuracy With a Reduced Computational Burden," *IEEE Transactions on Signal Processing*, vol. 43, no. 5, pp. 1232–1242, May 1995.
- [13] B. D. Rao and K. V. S. Hari, "Performance Analysis of Root-MUSIC," *IEEE Transactions on Acoustics, Speech, and Signal Processing*, vol. 37, no. 12, pp. 1939–1949, Dec 1989.
- [14] H. Krim, P. Forster, and J. G. Proakis, "Operator Approach to Performance Analysis of Root-MUSIC and Root-Min-Norm," *IEEE Transactions on Signal Processing*, vol. 40, no. 7, pp. 1687–1696, Jul 1992.
- [15] P. Stoica and A. Nehorai, "Performance Comparison of Subspace Rotation and MUSIC Methods for Direction Estimation," in *Fifth ASSP Workshop on Spectrum Estimation and Modeling*, Oct 1990, pp. 357–361.
- [16] M. Haardt, M. Pesavento, F. Roemer, and M. N. E. Korso, "Chapter 15 - Subspace Methods and Exploitation of Special Array Structures," in *Volume 3: Array and Statistical Signal Processing*, ser. Academic Press Library in Signal Processing, R. C. Abdelhak M. Zoubir, Mats Viberg and S. Theodoridis, Eds. Elsevier, 2014, vol. 3, pp. 651 – 717. [Online]. Available: <http://www.sciencedirect.com/science/article/pii/B9780124115972000151>
- [17] A. Paulraj, B. Ottersten, R. Roy, A. Swindlehurst, G. Xu, and T. Kailath, "Subspace Methods for Directions-Of-Arrival Estimation," *Handbook of Statistics*, vol. 10, pp. 693 – 739, 1993.

- [18] C. Vaidyanathan and K. Buckley, "Performance Analysis of the MVDR Spatial Spectrum Estimator," *Trans. Sig. Proc.*, vol. 43, no. 6, pp. 1427–1437, Jun. 1995.
- [19] M. Trinh-Hoang, M. Viberg, and M. Pesavento, "Improved DOA Estimators Using Partial Relaxation Approach," in *2017 IEEE International Workshop on Computational Advances in Multi-Sensor Adaptive Processing*, 2017.
- [20] M. Viberg and B. Ottersten, "Sensor Array Processing Based on Subspace Fitting," *IEEE Transactions on Signal Processing*, vol. 39, no. 5, pp. 1110–1121, May 1991.
- [21] B. Ottersten, M. Viberg, P. Stoica, and A. Nehorai, *Exact and Large Sample Maximum Likelihood Techniques for Parameter Estimation and Detection in Array Processing*. Berlin, Heidelberg: Springer Berlin Heidelberg, 1993, pp. 99–151.
- [22] I. Ziskind and M. Wax, "Maximum Likelihood Localization of Multiple Sources by Alternating Projection," *IEEE Transactions on Acoustics, Speech, and Signal Processing*, vol. 36, no. 10, pp. 1553–1560, Oct 1988.
- [23] P. Stoica and R. Moses, *Spectral Analysis of Signals*. Pearson Prentice Hall, 2005.
- [24] B. Ottersten, P. Stoica, and R. Roy, "Covariance Matching Estimation Techniques for Array Signal Processing Applications," *Digital Signal Processing*, vol. 8, no. 3, pp. 185 – 210, 1998.
- [25] J. Li, P. Stoica, and Z. Wang, "On Robust Capon Beamforming and Diagonal Loading," *IEEE Transactions on Signal Processing*, vol. 51, no. 7, pp. 1702–1715, July 2003.
- [26] T. Hayden and J. Wells, "Approximation by Matrices Positive Semidefinite on a Subspace," *Linear Algebra and its Applications*, vol. 109, pp. 115 – 130, 1988.
- [27] R. A. Horn, N. H. Rhee, and S. Wasin, "Eigenvalue Inequalities and Equalities," *Linear Algebra and its Applications*, vol. 270, no. 1, pp. 29 – 44, 1998. [Online]. Available: <http://www.sciencedirect.com/science/article/pii/S0024379597000311>
- [28] R. Burden and J. Faires, "Numerical analysis." Cengage Learning, 2010, pp. 48–49. [Online]. Available: <https://books.google.de/books?id=zXnSxY9G2JgC>
- [29] G. Golub and C. Van Loan, "Matrix Computations," ser. Johns Hopkins Studies in the Mathematical Sciences. Johns Hopkins University Press, 2012, ch. 8, pp. 439–494.
- [30] J. R. Bunch, C. P. Nielsen, and D. C. Sorensen, "Rank-One Modification of the Symmetric Eigenproblem," *Numerische Mathematik*, vol. 31, no. 1, pp. 31–48, 1978. [Online]. Available: <http://dx.doi.org/10.1007/BF01396012>
- [31] G. Golub and C. Van Loan, "Matrix Computations," ser. Johns Hopkins Studies in the Mathematical Sciences. Johns Hopkins University Press, 2012, pp. 469–471.
- [32] R.-C. Li, "Solving Secular Equations Stably and Efficiently," EECS Department, University of California, Berkeley, Tech. Rep. UCB/CSD-94-851, Dec 1994. [Online]. Available: <http://www2.eecs.berkeley.edu/Pubs/TechRpts/1994/5882.html>
- [33] A. Melman, "A Numerical Comparison of Methods for Solving Secular Equations," *Journal of Computational and Applied Mathematics*, vol. 86, no. 1, pp. 237 – 249, 1997, dedicated to William B. Gragg on the occasion of his 60th Birthday. [Online]. Available: <http://www.sciencedirect.com/science/article/pii/S037704279782122X>
- [34] S. A. Vorobyov, "Chapter 12 - Adaptive and Robust Beamforming," in *Volume 3: Array and Statistical Signal Processing*, ser. Academic Press Library in Signal Processing, R. C. Abdelhak M. Zoubir, Mats Viberg and S. Theodoridis, Eds. Elsevier, 2014, vol. 3, pp. 503 – 552. [Online]. Available: <http://www.sciencedirect.com/science/article/pii/B9780124115972000126>
- [35] Y. H. Hu, "Chapter 18 - Source Localization and Tracking," in *Volume 3: Array and Statistical Signal Processing*, ser. Academic Press Library in Signal Processing, R. C. Abdelhak M. Zoubir, Mats Viberg and S. Theodoridis, Eds. Elsevier, 2014, vol. 3, pp. 799 – 817. [Online]. Available: <http://www.sciencedirect.com/science/article/pii/B9780124115972000187>
- [36] K. Fan, "On a Theorem of Weyl Concerning Eigenvalues of Linear Transformations I," *Proceedings of the National Academy of Sciences*, vol. 35, no. 11, pp. 652–655, 1949. [Online]. Available: <http://www.pnas.org/content/35/11/652.short>
- [37] J. R. Magnus, "On Differentiating Eigenvalues and Eigenvectors," *Econometric Theory*, vol. 1, no. 2, pp. 179–191, 1985.